

Analysing the impact of large mammal herbivores on vegetation structure in Eastern African savannas combining high spatial resolution multispectral remote sensing data and field observations

Helena M. Back ^{a,*}, Isabel Pérez-Postigo ^a, Clemens Geitner ^b, Almut Arneth ^{a,c}

^a Karlsruhe Institute of Technology (KIT), Institute of Meteorology and Climate Research-Atmospheric Environmental Research (IMK-IFU), Garmisch-Partenkirchen, Germany

^b University of Innsbruck, Department of Geography, Innsbruck, Austria

^c Karlsruhe Institute of Technology (KIT), Institute of Geography and Geoecology (IfGG), Karlsruhe, Germany

ARTICLE INFO

Keywords:

GLCM texture measures
NDVI
PlanetScope
Sentinel-2
Savanna ecosystems
Exclusion experiments

ABSTRACT

It is well understood, that grazing and browsing in the African savanna ecosystem modulates tree-grass ratios. However, many of the large mammals are under pressure due to land use and climate change. It is challenging to predict how their altered abundance or range shifts will interact with savanna structure. Herbivore exclusion experiments can help to better understand the impacts of herbivores of different sizes on vegetation structure and composition, including interactions with rainfall. Here, we combine field data of the Ungulate Herbivory Under Rainfall Uncertainty (UHURU) exclusion experiment and high spatial resolution satellite images of the PlanetScope and Sentinel-2 series to investigate the impacts of herbivores on vegetation structure in a Kenyan savanna. Field data as well as NDVI values derived from Sentinel-2 and NDVI contrast values of PlanetScope show that presence of herbivores lowers vegetation cover and modify the woody vegetation structure depending on which herbivores are present. The vegetation grew tallest when mega-sized herbivores were absent but meso-sized and small herbivores were present, which resulted in high NDVI contrast values. The absence of herbivores resulted in fewer bare ground patches and increased green biomass, such as a higher mean canopy width, which led to higher NDVI values. Few studies have explored the potential of passive remote sensing data to assess herbivory impacts beyond the plot scale and over longer time-periods; however, these previous studies solely focused on the NDVI. Here we demonstrate the added value of also using GLCM texture measures to investigate effects on a savanna ecosystem in response to presence or absence of herbivores. Combining these data with plot measurements our study demonstrates the benefits of combining field and space perspectives in ecosystem studies.

1. Introduction

Savannas are ecosystems composed of a mosaic of trees and grasses. Their vegetation structure and composition are controlled to a variable degree by the amount and seasonality of rainfall, availability of soil nutrients, fire regime and herbivory (Staver et al., 2011). Savannas have a unique biodiversity and contribute notably to today's global land carbon sink (Ahlström et al., 2015; Friedlingstein et al., 2023; Searchinger et al., 2015). Herbivores have been shown to interact with carbon cycling in savanna ecosystem in complex ways (Daskin et al., 2016; Davies and Asner, 2019). Especially on the African continent, where many large mammal herbivores still remain, these act as important ecosystem engineers by removing a large proportion of the green

biomass both in the grass and tree layers (Asner et al., 2009; Goheen et al., 2018; Ripple et al., 2015; Sankaran et al., 2008; Staver et al., 2021; Wigley-Coetsee et al., 2022). Nevertheless, many of the large mammal populations are under pressure (Gobush et al., 2021; Rubenstein et al., 2016) due to poaching (Ripple et al., 2015), and habitat loss (Ogutu et al., 2017). Climate change and increasing atmospheric CO₂ are likely to alter savanna vegetation, impacting habitats for grazers and browsers. Warmer temperatures, changing rainfall patterns, and higher CO₂ concentrations will affect the competition between C3 and C4 plant species, thereby influencing the balance between grassy and woody vegetation (Bond and Midgley, 2012; Buitewerf et al., 2012).

A widely used method to assess the landscape and vegetation changes due to herbivory are exclusion experiments (Goheen et al.,

* Corresponding author.

E-mail address: helena.back@kit.edu (H.M. Back).

2018; Nasseri et al., 2011; Young et al., 1997). At plots in Kruger National Park, for instance, exclusion of large mammals led to woody vegetation growing taller and also to greater foliage height diversity compared to control sites (Levick et al., 2009). Similar results were found by Kibet et al. (2021) in Kenya, where *Acacia* sp. grew higher and woody biomass increased when browsing pressure was reduced. Generally, saplings suffer from herbivory and, as a result fewer trees reach the adult stage (Kibet et al., 2021). Sorokina et al. (2024) demonstrated that elephants can significantly alter tree structure using terrestrial laser scanning. Their study found that the tree height to crown length ratio was smaller in areas where elephants were more abundant. Furthermore, fire and rainfall, alongside herbivory, play a significant role in shaping the vegetation of the savanna (February et al., 2013; Staver et al., 2011; Staver et al., 2021). Understanding the complex interplay between these factors is key to grasping the dynamics of savanna ecosystems. Grass growth, which is highly sensitive to rainfall, not only fuels fires but also limits tree expansion (February et al., 2013). Herbivores further restrict the growth of both grasses and trees, with their impact being most pronounced at around 650 mm of annual rainfall (Staver et al., 2021). Rainfall enhances net primary production which correlates well with herbivore abundance (Coe et al., 1976). As rainfall increases (above 650 mm), the quality of forage diminishes, thus also reducing herbivory (Staver et al., 2021). However, rainfall can also limit the abundance of grazers; Georgiadis et al. (2007) found that rainfall can be limiting to the density of plains zebra (*Equus burchelli*). While these interactions are broadly understood, a more quantitative understanding of the impacts arising from presence or absence of animals in space and time remains challenging. Climate change will further increase the complexity. The balance of grazers, mixed feeders, and browsers likely plays a crucial role in maintaining a stable ecosystem, particularly in response to reduced rainfall (Irob et al., 2024). For example, Irob et al. (2024) used an ecohydrological model to study how vegetation responds to climate change and different herbivore regimes. Their results showed that savanna ecosystems were most stable across various climate scenarios when mixed feeders and browsers predominated, whereas intensive grazing led to ecosystem degradation.

Remote sensing methods are an important tool to further assess herbivore impacts on savannas over large areas and several years, thus providing added-value to field observations (Asner et al., 2009; Goheen et al., 2018; Levick et al., 2009; Sorokina et al., 2024). Texture measures of spectral data have been shown to be a reliable predictor for habitat heterogeneity and foliage height diversity (Petrou et al., 2012). For example, Wood et al. (2012) found a correlation between image textures and foliage height diversity in an oak savanna. These measures can also be used to predict habitat suitability for other species, e.g., birds (Farwell et al., 2021). Furthermore, Wood et al. (2012) showed that high spatial resolution of remote sensing information has important advantage in savannas where the vegetation is characterized by abrupt changes from tree patches to grassy patches. There is an abundance of satellite imagery available, much of it open-source, which highlights the immense potential of passive remote sensing techniques to extend fieldwork, fill data gaps, and advance studies on the interactions between herbivores and plants.

Few studies have explored the potential of combining high spatial resolution multispectral satellite images with in-situ vegetation data from herbivore exclusion plots. Most existing research has focused solely on the Normalized Difference Vegetation Index (NDVI; Goheen et al., 2013; Charles et al., 2017). In this study, we aim to utilize PlanetScope data, made available for the tropics through the Norway's International Climate and Forests Initiative Satellite Data program (NICFI) (NICFI, 2022), combined with data from Sentinel-2. By combining NDVI with NDVI contrast (Haralick et al., 1973) we extend the study of herbivore impacts from “greenness” (a surrogate for leaf biomass and photosynthesis) to measures that reflect impacts on canopy structure (and hence on the ecosystem more broadly). We retrieve texture measures and evaluate the changes in the plots of the Ungulate Herbivory Under

Rainfall Uncertainty experiment (UHURU) (Goheen et al., 2013) plots, jointly with field data from Alston et al. (2022). We assess 1) the effects of herbivore activity on canopy width, height and structural diversity. And we explore 2) if the herbivore impacts can be assessed based on multi-temporal satellite data, despite large seasonal and interannual variability in rainfall patterns in the semi-arid ecosystems.

2. Materials and methods

2.1. Study area

The UHURU experimental plots are located at the Mpala Ranch and Research Center (MRC) in Laikipia, Kenya ($0^{\circ}17'N$, $37^{\circ}52'E$, 1600 m elevation). The terrain in the area is hilly with altitudes between 1500 m a.s.l and 1830 m a.s.l. The sandy loam soils are well drained (Ahn and Geiger, 1987). After Olson et al. (2001) the MRC is located in the ecoregion defined as tropical and subtropical grasslands, savannas, and shrublands. The climate is semi-arid (~ 440 to 640 mm precipitation/year) with two rainy seasons from March to May (long rainy season) and October to November (short rainy season) (Alston et al., 2022; Augustine and McNaughton, 2004). The woody vegetation is dominated by *Acacia (Senegalia) mellifera*, *Acacia (Vachellia) etbaica*, and *Acacia (Senegalia) brevispica*. In the grass layer, dominant species are e.g. *Pennisetum stramineum* and *Cynodon dactylon* (Augustine, 2003). Mammal herbivores include small species e.g., dik-dik (*Madoqua cavendishi*) and warthog (*Phacochoerus africanus*), meso-sized herbivores, e.g., impala (*Aepyceros melampus*) or zebra (*Equus spp.*) and mega-sized herbivores, e.g., elephant (*Loxodonta africana*) and giraffes (*Giraffa camelopardalis*) (Goheen et al., 2013). At the MRC, a private conservancy, cattle ranching, and wildlife coexist (Kibet et al., 2021; Young et al., 1997).

The three exclosures sites of UHURU are distributed from north to south, at three locations where soil and rainfall differs (Fig. 1, Table 1). At every location, four different treatment plots of a size of $100\text{ m} \times 100\text{ m}$ are implemented excluding herbivores of different sizes. The closed plots (LMH) exclude all herbivores taller than 50 cm, but still accessible for e.g. hares (*Lepus spp.*). MESO plots exclude all meso-sized herbivores larger than 120 cm, hence the main browser is the dik-dik (Goheen et al., 2013). In the MEGA plots giraffes and elephants are excluded but impalas, zebras, and small herbivores can enter. Lastly, control plots (CTL) are unfenced and accessible to all herbivores except cattle, which herders are asked to keep from entering the plots (Goheen et al., 2013). For more details to the experiment set up, refer to Goheen et al. (2013). The experiment was established in 2008 and is still ongoing.

2.2. Data description

2.2.1. PlanetScope data

PlanetScope data (Planet Labs PBC, 2020–2023) was accessed through the Norway's International Climate and Forests Initiative Satellite Data program (NICFI), a fund giving access to high spatial resolution PlanetScope surface reflectance data in the tropical regions between 30 degrees north and 30 degrees south (Pandey et al., 2021). The images have a spatial resolution of 4.77 m and four spectral bands (Red (R), Green (G), Blue (B), and Near Infrared (NIR)). The NICFI program offers one image mosaic covering the entire tropical belt per month since September 2020. The mosaics are stacked together with selected scenes of the month, and usually are from different dates due to atmospheric artefacts (e.g., clouds). Due to this temporal inconsistency, the images we used for individual locations at UHURU can be from different days within the month. In this study, we used data covering the three-year time period from September 2020 to August 2023.

2.2.2. Sentinel-2 data

We used images from the multispectral sensors of Sentinel-2 A and -2B (level 2 A), which were available from 2019 on the Google Earth Engine cloud. The combined revisit time of the two Sentinel-2 satellites

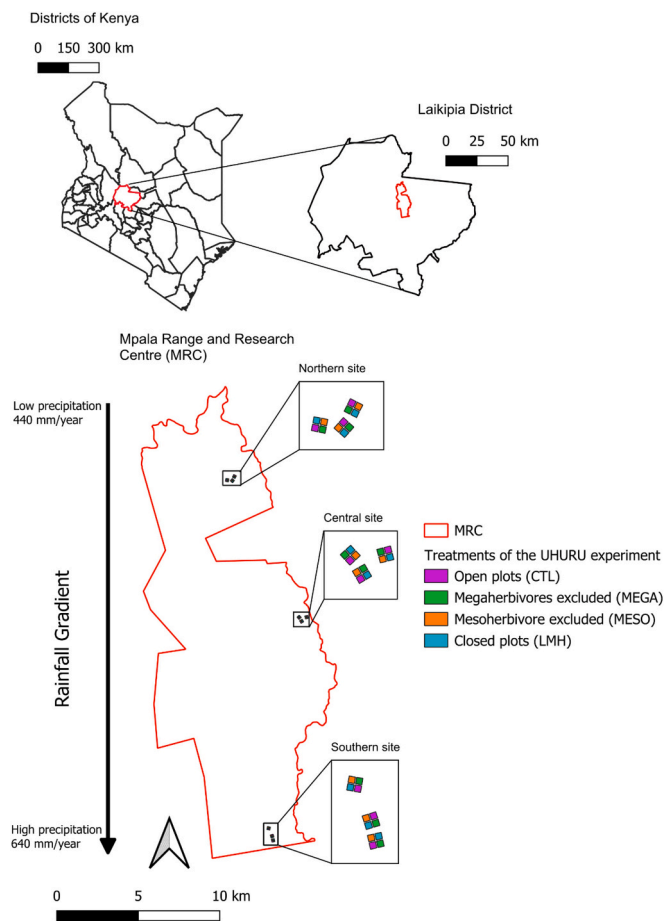


Fig. 1. Location of the Mpala Ranch Research Centre in Kenya (above) and the experimental site and plot design (below).

Table 1

Annual rainfall from 2015 to 2023 derived from the CHIRPS dataset. The study period is colored dark grey.

Year	UHURU north [mm/year]	UHURU central [mm/year]	UHURU south [mm/year]
2015	272	317	360
2016	389	464	632
2017	423	495	673
2018	781	927	1148
2019	667	789	1040
2020	754	867	1112
2021	425	496	656
2022	380	456	580
2023	578	685	873

is 5 days. We used the R (Band 4) and NIR (Band 8) bands from the level 2 A product, which provides atmospherically corrected data representing bottom-of-atmosphere reflectance. Both bands used in this study (R and NIR) have a high spatial resolution of 10 m (Drusch et al., 2012; Szantoi and Strobl, 2019). We selected Sentinel-2 images from September 2020–August 2023 to match the availability of PlanetScope data. Only images with a cloud cover <10 % were considered for our analysis, resulting in 84 images. Additionally, a cloud mask was applied to remove pixels affected by clouds.

2.3. Field data

From the very beginning of the exclosure experiments in 2008 until 2019 vegetation data from field campaigns are available (Alston et al.,

2022). For this study the data from 2016 onward was used. Vegetation response to changes in herbivory develops over several years. For instance, Augustine and McNaughton (2004) implemented twelve 0.5 ha exclusion plots and twelve 0.5 ha control plots at the MRC and detected an increase in woody biomass within the first three years of exclusion. Wigley et al. (2020) observed a continued increase in woody biomass during the first ten years of the same exclusion experiment, driven by seedling regrowth until competition eventually led to stabilization. Hence our choice seems appropriate to compare field observations from eight years after the start of the experiment to the satellite data. Due to data availability, there is a temporal mismatch between the field data selected from Alston et al. (2022), which covers the years 2016–2019, and the satellite images (2020–2023) from the PlanetScope imagery under the NICFI program. However, we are interested in differences between plots and thus consider the observed patterns related to herbivore impacts, seasonality, and rainfall response to be comparable. Alston et al. (2022) monitored biannually 49 quadrats of 1 m² within each plot of the experiment, to represent the whole 100 m × 100 m plot. We used data from the understory surveys, providing information about herbaceous species abundance, and the percentage of bare ground in the plots. We found the understory data-set useful in this ecosystem, since the canopy is open and sparse, thus satellite images can detect a signal from the understory as well. Additionally, we used the measured vertical vegetation data of all vegetation layers to obtain information about the vegetation structure, as well as measurements of the canopy height and width of trees. Trees above 0.05 m height were measured. For more details on the measurements please refer to Alston et al. (2022). We chose these characteristics of the vegetation in order to investigate which structural metrics (e.g., canopy height median, canopy SD) correlate with the NDVI and NDVI contrast.

2.3.1. CHIRPS data

The CHIRPS data represents a high-spatial and high-temporal resolution precipitation dataset. By combining satellite data and in-situ rain gauges it estimates daily rainfall events with a spatial resolution of 0.05° (Funk et al., 2015). This allowed to download separate rainfall estimates for every UHURU location for the study period (September 2020 – August 2023). Additionally, we compared our study years to previous years, to assess whether the years are rather dry or wet.

2.4. Data processing

2.4.1. Processing of the remote sensing data

PlanetScope and Sentinel-2 data were accessed and processed in Google Earth Engine (GEE) (Gorelick et al., 2017). The dense time-series of Sentinel-2 was used to assess the vegetation cover using the NDVI. The high spatial resolution of the PlanetScope data was advantageous to characterize the vegetation structure on the basis of the NDVI contrast, because of its high spatial resolution. Calculating the NDVI for the PlanetScope data did not provide additional benefits, as it did not significantly increase the density of the time series. Conversely, the lower resolution of Sentinel-2 images did not offer further insights from NDVI contrast. We used a shapefile of the exclusion plots using coordinates provided by Alston et al. (2022) to spatially match the satellite imagery. We applied a buffer of –8 m to the shapefiles of the experimental plots to exclude pixels that straddled adjacent plots and minimise potential boundary effects. The NDVI, first described by Rouse et al. (1974), of the Sentinel-2 images was used to estimate the difference in greenness between the plots. The NDVI is calculated using the values of the NIR and Red bands. The higher the photosynthetic rate, which is linked to plant green biomass, the higher the reflection in the NIR spectrum and the lower in the Red (Hoffer and Johannsen, 1969; Huete et al., 1994). We calculated mean values of NDVI pixel values per plot (Gordijn et al., 2012; Petrou et al., 2012). Outliers (values in the 5th and 95th percentiles) were not considered for further analysis.

The NDVI contrast was calculated to estimate the structural

heterogeneity of the vegetation using the NDVI of the PlanetScope data, since it has a higher spatial resolution.

The Grey Level Co-Occurrence matrix (GLCM), a method developed by Haralick et al. (1973), quantifies the relationship of pixel values (here, NDVI) among neighbouring pixels. Because only one PlanetScope image per month was available, one NDVI contrast value per month per plot was calculated. The higher the NDVI contrast in a pixel, the higher the difference to its defined neighbourhood:

$$\text{NDVI contrast} = \sum_{i,j=0}^{N-1} P(i,j)(i-j)^2$$

where N is the number of image grey levels (here NDVI), i is the row and j the column number of the GLCM, and p the probability for the cell (i,j) .

The neighbourhood defined here had a kernel size of 3×3 pixels (pixel size $4.77 \text{ m} \times 4.77 \text{ m}$). This means that the pixel of interest will only be compared to its direct focal neighbours but not to a larger area. There are some assumptions behind using the NDVI contrast to estimate structural diversity. First, the spectral diversity hypothesis, that different species have different signals in the red and infrared, and thus influence the NDVI value of a cell (Kacic and Kuenzer, 2022, Torresani et al., 2024). Second the structure of the cells will influence the NDVI value:

Depending on the vegetation types and the percent of bare ground the NDVI differs within one cell. A pixel containing a small shrub will have a lower NDVI than a pixel with a larger tree or more grass in it. Thus, changes from cell to cell indicate a change in the vegetation's structure, as demonstrated by Wood et al. (2012) who tested this method in different savanna ecosystems. Previous studies have shown that the NDVI contrast correlates with the vegetation structure (Farwell et al., 2021; Fundisi et al., 2020; Wood et al., 2012). Following the workflow by Gordijn et al. (2012), Petrou et al. (2012), and Wood et al. (2012), we calculated the mean NDVI pixel values and mean NDVI contrast pixel values for each treatment (CTL, MEGA, MESO, LMH) in each location (north, central, south).

2.4.2. Processing of the field data

The field observation data from Alston et al. (2022) were compared with the results of the remote sensing analyses. For details about the field sampling protocol refer to Alston et al. (2022). The percentage of bare ground in the monitored quadrats (49 per plot) was averaged across time for each plot, to have one value for each $100 \text{ m} \times 100 \text{ m}$ plot. Mean canopy width and mean canopy height were calculated for every treatment plot at each of the three locations. Since the NDVI contrast can be a proxy for the diversity in the vertical vegetation, the median height of the vegetation layers and the standard deviation (SD) of the height of the vegetation layers were calculated. Lastly, the Shannon-Diversity Index (SDI) was calculated for the tree species and understory species:

$$H' = - \sum_{i=1}^s p_i \ln(p_i)$$

$$p_i = \frac{n_i}{N}$$

where H' is the species diversity index, s is the number of species, n_i is the number of individuals of species i and N is the number of individuals of all species. Consequently, p_i is the proportion of species I in the given community (Shannon, 1948).

2.5. Statistical analysis

We assessed the data (NDVI and NDVI contrast values) for normality using the Shapiro-Wilk test ($p < 0.0001$). As the null hypothesis of a normal distribution was rejected the Spearman's rank correlation was computed, in order to investigate the relationship between the per-plot averaged field measures and the remote sensing measures. The relationship between the NDVI mean of each plot and the mean value of the

NDVI contrast was compared to the field measures (SDI understory, SDI trees, percentage of bare ground, vertical vegetation SD, vertical vegetation median, canopy width mean).

To investigate the response of the NDVI and NDVI contrast to treatments and locations, we fitted generalized mixed models using the *lme4* (Bates et al., 2015) package in R (R Core Team, 2023). The response variables were the NDVI and NDVI contrast, with treatment and location as fixed effects. Blocks were included as a random effect to account for replicate block variability. As the null hypothesis of a normal distribution was rejected, we proceeded with a generalized mixed model, testing different families and link functions. For both NDVI and NDVI contrast, we selected the model with the lowest Akaike Information Criterion (AIC). The best model for NDVI was found to be from the gamma family with the identity link function, while for the NDVI contrast, the inverse Gaussian family with the identity link function provided the best fit. As a post-hoc analysis, we performed Dunnett's test and tested each location separately, as we observed significant location effects on NDVI contrast for northern and southern location and on NDVI for the southern location. We considered a p -value of 0.001 as significant.

3. Results

The CHIRPS data shows that the years of the study period (09/2020–09/2023) were drier compared to the years immediately before (2018–2020) but were well within the interannual variability in the region (e.g., example years from 2015, Table 1).

3.1. Herbivore impacts as reflected by the NDVI mean

The results of the generalized mixed model testing the NDVI with the lowest AIC ($\text{AIC} = -5629$) showed that every treatment has an effect on the NDVI compared to the CTL plots ($\beta_{LMH} = 0.14$, $\beta_{MEGA} = 0.05$, $\beta_{MESO} = 0.09$, p -values <0.0001) and that the southern location has an effect compared to the central blocks ($\beta = 0.05$, p -value <0.0001) but the northern location does not ($\beta = 0.1$, p -value >0.1). The mean NDVI time series of the Sentinel-2 images (Fig. 2) shows - with few exceptions - the differences between the treatments in both wet and dry seasons. Additionally, the effects of the MEGA ($\beta = -0.05$, p -value <0.0001) and MESO ($\beta = 0.03$, p -value <0.001) treatments were influenced by the northern location, suggesting an interaction between the treatments and this location. At the southern location the LMH treatment was influenced by the location ($\beta = 0.02$, $p < 0.05$).

In general, mean NDVI values were positively correlated with the degree of herbivore exclusion. The CTL (open) plots exhibited the lowest mean NDVI values throughout the study period, whereas the LMH (closed) plots demonstrated the highest mean NDVI values, followed by the MESO and MEGA plots. However, there were some exceptions, for example at the northern plots in the first two years of this study values in the MESO and MEGA plots were comparable, while at the southern location the MESO plots had on some occasions higher NDVI values than the LMH plots (Fig. 2). The results of the post-hoc Dunnett's test on statistical difference are displayed in Fig. 4 and are separated for each location. At the northern location, all treatment combinations showed significant differences ($p < 0.001$), except for LMH and MESO ($p = 0.0357$) and MEGA and MESO ($p = 0.0014$), which were also significant but at a higher p -value. The central treatments were all significant ($p < 0.0001$), whereas at the southern location we did not find a difference between LMH and MESO plots ($p = 0.0881$). The results of the Spearman's rank analysis indicate that the mean percentage of bare ground from the field data is the primary factor contributing to the observed difference in NDVI mean values ($r = -0.64$, $p < 0.0001$). Presence of herbivores led to larger areas of bare ground in the plots (Figure S1). A weak positive correlation was also found between canopy width and the NDVI mean ($r = 0.47$, $p = 0.0038$). The correlations between NDVI and SDI of understory and trees were not significant ($r = 0.04$, $p = 0.83$, $r = 0.05$, $p = 0.74$, respectively).

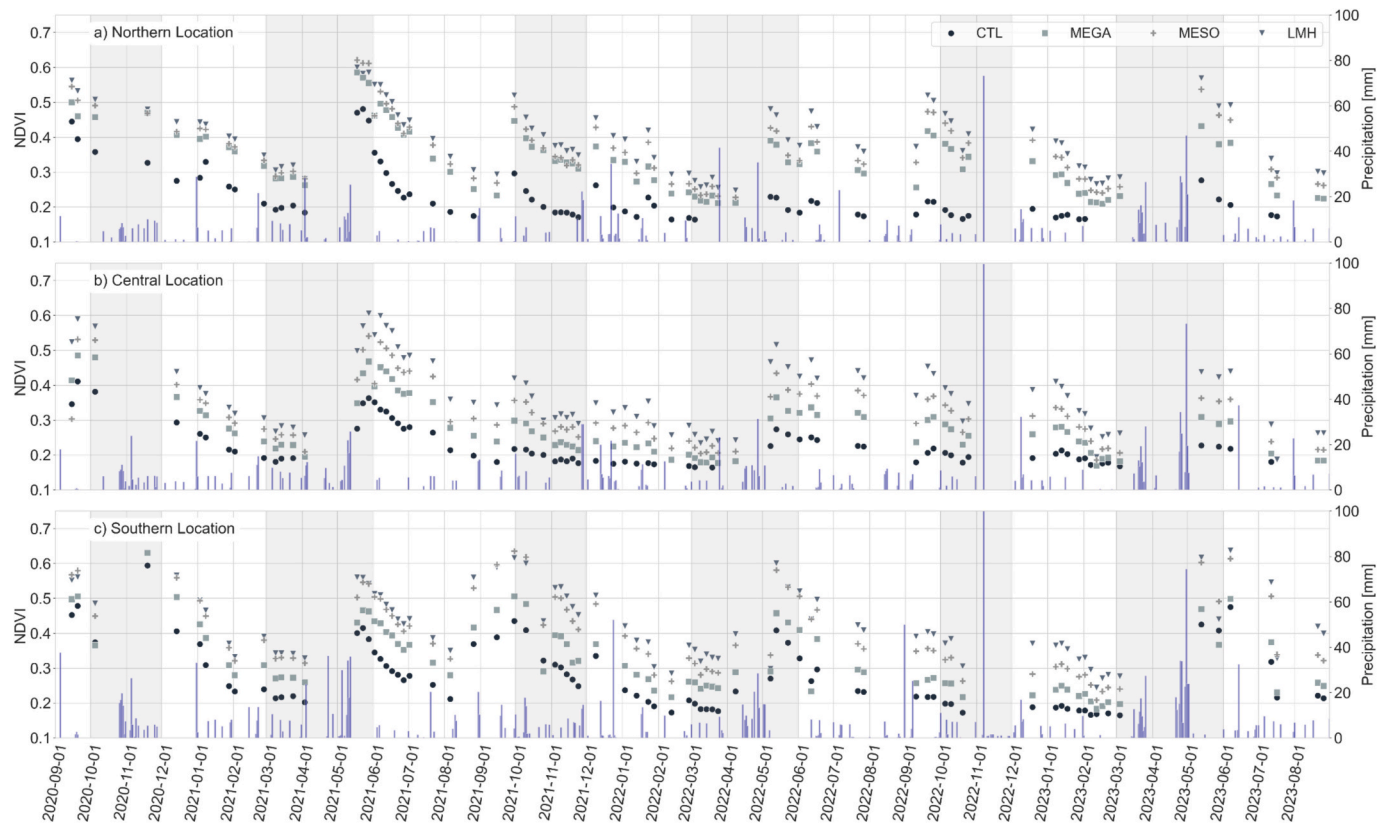


Fig. 2. NDVI time series of the Sentinel-2 data and daily rainfall for the a) northern location, b) central location, c) southern location. For every date the NDVI mean within one treatment is calculated. The typical rainy seasons, according to the literature, are colored in grey. Blue bars show daily rainfall. (For interpretation of the references to colour in this figure legend, the reader is referred to the web version of this article.)

3.2. Herbivore impacts as reflected by the NDVI contrast

The best model for the NDVI contrast (AIC = 11,274) showed significant effects on the response variable and interactions between treatments and locations. It revealed that the MEGA and MESO treatments differ from the CTL plots ($\beta_{MEGA} = 15.52$, $\beta_{MESO} = 21.4$, $p < 0.001$) whereas the model did not identify significant effects of the LMH treatment. The northern and southern location had an effect on the NDVI contrast ($\beta_{\text{N}} = -10.97$, $p < 0.0001$, $\beta_{\text{S}} = -11.25$, $p < 0.0001$, respectively). Especially at the northern location the effect of the NDVI contrast in the MEGA and LMH plots was amplified ($\beta_{MEGA} = 27.85$, $p < 0.0001$, $\beta_{LMH} = 10.17$, $p < 0.05$). The Dunnett's test further confirmed the strong effect of location (Fig. 5). At the northern location the NDVI contrast differed among treatments ($p < 0.0001$) except between the LMH and MESO treatments ($p = 0.9452$). At the central location, there was a statistically significant difference between the CTL and MESO plots ($p < 0.0001$) only, while the differences between CTL and MEGA ($p = 0.0012$) and LMH and MESO ($p = 0.0077$) were not as pronounced. At the southern location, significant differences were observed between the CTL and LMH plots ($p < 0.001$), between the CTL and MEGA plots ($p < 0.0001$), and between the MEGA and MESO plots ($p < 0.001$). To conclude, while treatments influenced the NDVI contrast throughout the experiment, the locations had a strong impact, and the treatment effect was not consistently prominent.

The NDVI contrast (Fig. 3) was highest in the MEGA plots, followed by the MESO plots. CTL and LMH plots had the lowest values. This finding is corroborated by the field observations: median height and SD of the vertical vegetation layers tended to be highest in the MEGA plots and second in the MESO plots over all locations (Figure S1). Vertical and horizontal vegetation structure correlates well with the NDVI contrast (e.g., vertical vegetation median height and standard deviation height

and canopy width, $r = 0.64$ – 0.66 , $p < 0.0001$, Table 2, Figure S2). However, the NDVI contrast also differed from the general patterns in some locations and points in time, similar to what was also observed in the NDVI data. At the central site, NDVI contrast in the MESO plots was sometimes as high or even higher than the NDVI contrast values found in the MEGA plots, especially in 2022 and 2023 (Fig. 3). This stands in contrast to the field data that showed substantial differences in median vegetation layer height, and the height SD, between the MEGA and MESO plots at the central location. No correlation was found between the NDVI contrast and the SDI of the understory ($r = -0.17$, $p = 0.33$), between NDVI contrast and SDI of trees ($r = -0.23$, $p = 0.18$) and between NDVI contrast and the bare ground ($r = 0.25$, $p = 0.15$).

4. Discussion

We used the NDVI and NDVI contrast as proxies for the biomass and structure of the vegetation and our results confirm the impact of large mammal herbivores on both in the Kenyan savanna. The NDVI showed a difference between the treatments whereas the NDVI contrast of the treatments differed from the CTL plots but could not always distinguish between the treatments. In 2009, Goheen et al. (2013) explored the UHURU plots using the NDVI of the Quickbird satellite image finding similar results. The NDVI increased with the degree of herbivore exclusion from a plot, and could therefore be used to distinguish between the treatments. Herbivore impact at UHURU was detectable throughout the entire study period of this study, irrespective of rainfall seasonality. Nevertheless, all treatments showed a strong seasonal pattern, having higher NDVI mean values at the end and after rainy periods. However, at the northern and southern location the MESO and LMH treatments were not distinguishable. Unfortunately, NDVI mean values during the rainy season are mostly lacking because in this time



Fig. 3. The NDVI contrast for every month of the PlanetScope images at the a) northern location, b) central location, c) southern location. The mean of the NDVI contrast is shown for every treatment. The typical rainy seasons, according to the literature, are colored in grey.

Table 2

Results of the spearman's rank correlation, r - and p -values. See also Fig. S2.

Measure	SDI understory	SDI trees	Bare ground [%]	Vertical vegetation SD	Vertical vegetation median	Canopy width mean
NDVI mean (Sentinel-2)	$r = 0.04$ $p = 0.83$	$r = 0.05$ $p = 0.74$	$r = -0.64$ $p < 0.0001$	$r = 0.15$ $p = 0.37$	$r = 0.06$ $p = 0.65$	$r = 0.47$ $p = 0.004$
NDVI contrast (PlanetScope)	$r = -0.17$ $p = 0.33$	$r = -0.23$ $p = 0.18$	$r = 0.25$ $p = 0.15$	$r = 0.64$ $p < 0.0001$	$r = 0.66$ $p < 0.0001$	$r = 0.66$ $p < 0.0001$

cloud free images are rarely available.

The NDVI contrast effectively identified the more diverse vegetation structure in the MESO and MEGA plots. Previous studies have demonstrated the suitability of the NDVI contrast to investigate the vegetation structure: [Wood et al. \(2012\)](#) found the NDVI contrast to be associated with the diversity of horizontal woody structure in woodland, grassland and savanna ecosystems. [Farwell et al. \(2021\)](#) reached similar results in

forests, grasslands and shrublands across the US. Another study ([Dos Reis et al., 2020](#)) used the NDVI contrast of the PlanetScope satellites to successfully estimate canopy height and above ground biomass in pastureland in Brazil. In this study we found significant correlations between measures of the canopy width and vertical vegetation SD and the NDVI contrast.

The spatial resolution of about 4.77 m of the PlanetScope data was

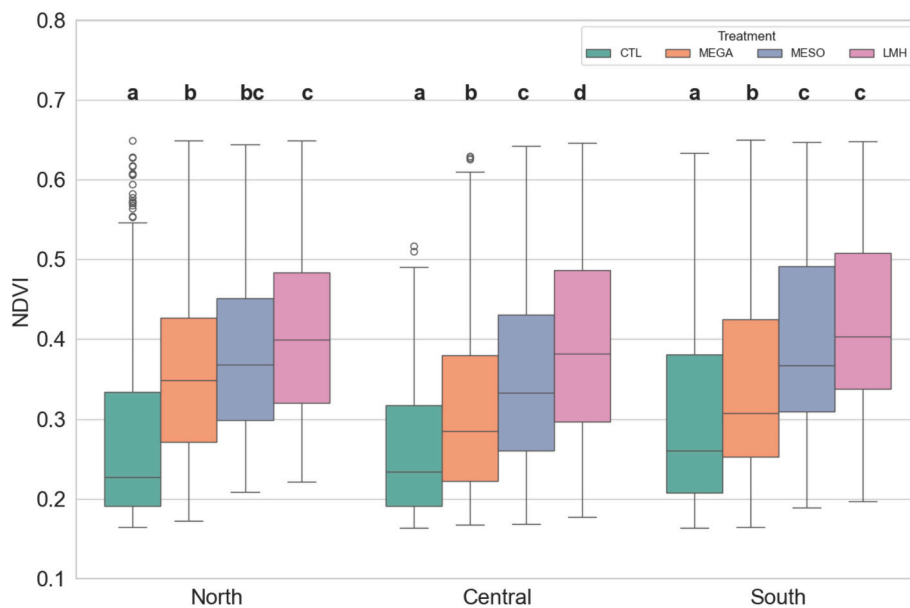


Fig. 4. Effects of the NDVI mean values on the treatments in each location (Dunnett's test). Statistical significance is based on a *p*-value of 0.001. Boxplots show the interquartile range (boxes), median (central line), 1.5 x interquartile range (whiskers) and outliers (points).

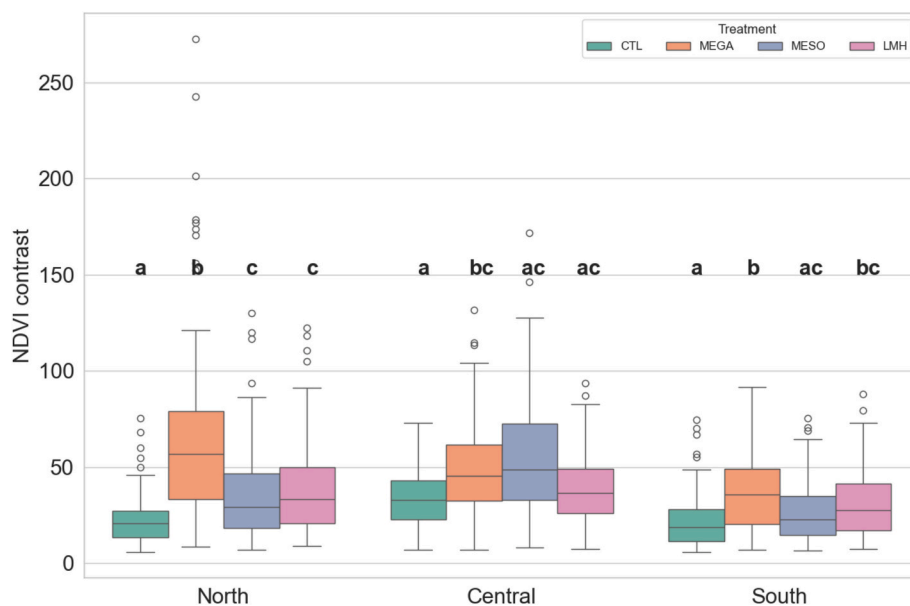


Fig. 5. Effects of the NDVI contrast mean values on the treatments in each location (Dunnett's test). Statistical significance is based on a *p*-value of 0.001. Boxplots show the interquartile range (boxes), median (central line), 1.5 x interquartile range (whiskers) and outliers (points).

high enough to capture the vegetation's structure. Although single plants or smaller patches do not cover whole pixels, their spectral information is still captured in relation to the relative abundance of trees and grasses therefore shown in the NDVI and NDVI contrast. Our study showed that contrast derived from GLCM texture can be a good method to derive vertical and horizontal structural information of the vegetation, as shown in previous studies described above (Dos Reis et al., 2020; Farwell et al., 2021; Wood et al., 2012). At the same time, Sentinel-2 imagery provided a dense time series of NDVI mean values as an indicator for photosynthetic activity. These remote sensing methods therefore are valuable tools for evaluating ecological experiments at the landscape scale. We additionally show the benefits of different sensors, as the Sentinel-2 sensor was valuable for a dense NDVI time series and the PlanetScope sensor was beneficial in the analysis of the vegetation

structure due to the high-spatial resolution.

Having access to the field data alongside the remote sensing measures allows us to evaluate the remote sensing results from a broader ecological perspective. The increasing NDVI values in exclusion plots goes hand in hand with the field-measured lower percentage of bare patches and the greater width of the canopy. Asner et al. (2009) found a similar correlation between degree of exclusion and percentage of bare ground in exclusion plots in the Kruger National Park using LiDAR data. Additionally, they found a denser woody cover inside the exclusion plots. An increase of greenness with absence of herbivory seems to be a robust pattern for the African savanna biome, as demonstrated by Sankaran et al. (2008) who found a negative relationship between the presence of browsers and woody biomass comparing data from savannas all over the African continent. Other studies (Fornara and Du Toit, 2008;

Kibet et al., 2021; Levick et al., 2009) observed reduced width and density of the canopy due to browsers. This indicates that the NDVI is an appropriate measure to detect the changes of the woody vegetation and the proportion of the bare ground in the UHURU plots.

Vegetation structure varied depending on which sizes of herbivores are present in the UHURU plots. In particular, the ground measurements in the MEGA plots indicated overall taller and also more variable (larger SD in the measured height) vegetation structure, compared to the other treatment plots (see Figure S1). These previous ground observations made in Goheen et al. (2013) were also reflected in recent measurements by Coverdale et al. (2024) who studied the UHURU plots using LiDAR and field measurements, and were also reflected in very high NDVI contrast values in this study. These impacts of herbivores on vegetation structure might be attributable to disparate feeding patterns (browsing or grazing) and different browse heights of different species. Elephants and giraffes can feed up to 4 m (Cameron and du Toit, 2007; O'Connor et al., 2015). In the MEGA plots where elephants and giraffes are absent, none of the herbivore species are able to consume the topmost layers of trees (> 2.5 m), which results in the increase in tree height. Similar observations were made by Augustine and McNaughton (2004), who installed exclusion plots at Mpala and observed that elephants particularly damaged tree layers above 2.5 m. This effect is further enhanced by meso-sized herbivores, for example the impala browsing at head height (~80 cm) (Mramba, 2021), taking away the biomass of lower layers, such that trees compensate the loss of biomass in the lower layers by growing taller (Fornara and Du Toit, 2008). Coverdale et al. (2024) showed that meso-sized and small-sized herbivores mainly modify the structure of shrubs. A similar effect was observed in the MESO plots using the NDVI contrast at the central site, although weaker. There, mainly the dik-dik occurs, a small browser that is capable of influencing vegetation structure and vegetational biomass by browsing saplings and twigs, especially in the understory (Coverdale et al., 2024). Augustine and McNaughton (2004) showed that the dik-dik can remove up to 63 % of the leaf area in their accessible height. However, the effect was not strong enough in the MESO plots at the northern and southern location to detect it with the NDVI contrast or the NDVI alone compared to the LMH plots. Elephants modify the structure of trees by altering the branch area and crown height (Sorokina et al., 2024), which aligns with the study of Coverdale et al. (2024) where they showed the strong effects of megaherbivores on structural complexity and mean canopy height. Additionally, the experimental studies of February et al. (2013) and Kambatuku et al. (2011) found that the removal of grasses due to the presence of grazers benefitted trees by increasing the availability of water and nutrients, which was probably the case in the MEGA plots. February et al. (2013) conducted an experiment in which they removed grass surrounding regrowing *Acacia (Senegalia) nigrescens* and *Terminalia sericea* after a fire. They found that grasses inhibit tree growth by competing for soil resources. In contrast, grasses were not negatively affected by the presence of trees and were primarily dependent on rainfall. Similarly, Kambatuku et al. (2011) demonstrated in a greenhouse experiment that grasses restrict tree growth. However, they found no evidence of nutrient deficiency in trees due to the presence of grasses.

By contrast to the MEGA, the woody vegetation structure (measured with vertical vegetation SD and NDVI contrast) in the CTL and LMH plots was much more homogeneous but likely for different reasons. In the CTL plots large bare patches and overall small trees result in many pixels with a low NDVI adjacent to each other, whereas the LMH plots are densely vegetated, with a high NDVI across all pixels. Consequently, in both cases structural heterogeneity of the vegetation and thus NDVI contrast is low.

In summary, the vegetation density and structure are significantly influenced by browsers and grazers: when fewer browsers are present (MEGA and MESO), trees can grow taller and the height layers become more diverse. Grazers remove the grasses, consequently more water and nutrients are available for the woody vegetation. However, when all herbivores are excluded (LMH), then the picture becomes more

homogenous again.

Exclusion plots may exhibit bias since the presence or absence of certain herbivores can influence the abundance of others. Small herbivores for example could prefer habitats where the vegetation is denser, due to the lack of megaherbivores, because those habitats are good shelters (Wells et al., 2021). Large-scale 'natural' experiments allow the results of

small-scale exclusion experiments to be interpreted in context of ecosystem level processes.

For instance, during the civil war in Mozambique, the decline of herbivores during the unrest contributed to less browsing pressure which resulted in higher sapling survival and tree growth (Daskin et al., 2016). Holdo et al. (2009) used a Bayesian state-space model to examine the interaction between herbivores and fire regimes in the savanna biome. They found that the recovery of the wildebeest population following the eradication of rinderpest led to an increase in tree cover. As the wildebeest population grew, they consumed more grasses, which reduced the fuel available for savanna fires. Consequently, the decreased fire frequency allowed more tree seedlings to grow tall enough to escape the typical flame height.

Additionally, it is important to mention that although we explore here the relationship between herbivory and vegetation also with regard to rainfall, the data does not allow us to address how climate change, particularly shifting fire regimes, may alter these interactions.

The design of the UHURU experiment allows the impact of herbivores of varying sizes to be studied. Given the difficulties of obtaining spatially replicated time-series of vegetation changes from field measurements alone, high-resolution imagery that can be supported by more infrequent ground observation seems a promising avenue to fill data gaps in remote areas.

Declaration of generative AI and AI-assisted technologies in the writing process

During the preparation of this work the author(s) used ChatGPT in order to check and improve the English grammar. After using this tool/service, the author(s) reviewed and edited the content as needed and take(s) full responsibility for the content of the publication.

CRediT authorship contribution statement

Helena M. Back: Writing – original draft, Methodology, Investigation, Conceptualization. **Isabel Pérez-Postigo:** Writing – review & editing, Supervision, Methodology, Conceptualization. **Clemens Geitner:** Writing – review & editing, Supervision. **Almut Arneth:** Writing – review & editing, Supervision, Conceptualization.

Declaration of competing interest

The authors declare that they have no known competing financial interests or personal relationships that could have appeared to influence the work reported in this paper.

Appendix A. Supplementary data

Supplementary data to this article can be found online at <https://doi.org/10.1016/j.ecoinf.2025.103113>.

Data availability

The codes to conduct the statistical analysis and replicate the figures, the NDVI data from the Sentinel-2 sensors, and the processed field data are available at <https://doi.org/10.5281/zenodo.15006724>. The original field data can be found in Alston et al., 2022 (<https://doi.org/10.1002/ecy.3649>). The texture measures of the PlanetScope data for the study area are stored at <https://doi.org/10.1016/j.ecoinf.2025.103113>.

[org/10.5281/zenodo.15011739](https://doi.org/10.5281/zenodo.15011739). CHIRPS data can be accessed here: <https://www.chc.ucsb.edu/data/chirps>.

References

Ahlström, A., Raupach, M.R., Schurgers, G., Smith, B., Arneth, A., Jung, M., Reichstein, M., Canadell, J.G., Friedlingstein, P., Jain, A.K., et al., 2015. The dominant role of semi-arid ecosystems in the trend and variability of the land CO₂ sink. *Science* 348, 895–899. <https://doi.org/10.1126/science.aaa1668>.

Ahn, P.M., Geiger, L.C., 1987. Kenya Soil Survey - Soils of Laikipia District. Ministry of Agriculture, National Agricultural Laboratories, Kenya Soil Survey.

Alston, J.M., Reed, C.G., Khasoha, L.M., Brown, B.R.P., Busienei, G., Carlson, N., Coverdale, T.C., Dudenhofer, M., Dyck, M.A., Ekeno, J., et al., 2022. Ecological consequences of large herbivore exclusion in an African savanna: 12 years of data from the UHURU experiment. *Ecol* 103, e3649.

Asner, G.P., Levick, S.R., Kennedy-Bowdoin, T., Knapp, D.E., Emerson, R., Jacobson, J., Colgan, M.S., Martin, R.E., 2009. Large-scale impacts of herbivores on the structural diversity of African savannas. *Proc. Natl. Acad. Sci.* 106, 4947–4952. <https://doi.org/10.1073/pnas.0810637106>.

Augustine, D.J., 2003. Spatial heterogeneity in the herbaceous layer of a semi-arid savanna ecosystem. *Plant Ecol.* 167, 319–332.

Augustine, D.J., McNaughton, S.J., 2004. Regulation of shrub dynamics by native browsing ungulates on East African rangeland. *J. Appl. Ecol.* 41, 45–58.

Bates, D., Mächler, M., Bolker, B., Walker, S., 2015. Fitting linear mixed-effects models using lme4. *J. Stat. Softw.* 67 (1), 1–48. <https://doi.org/10.18637/jss.v067.i01>.

Bond, W.J., Midgley, G.F., 2012. Carbon dioxide and the uneasy interactions of trees and savannah grasses. *Philosoph. Trans. Royal Soc. Lond. Ser. B Biol. Sci.* 367, 601–612. <https://doi.org/10.1098/rstb.2011.0182>.

Buitenhof, R., Bond, W.J., Stevens, N., Trollope, W.S.W., 2012. Increased tree densities in south African savannas: >50 years of data suggests CO₂ as a driver. *Glob. Chang. Biol.* 18, 675–684. <https://doi.org/10.1111/j.1365-2486.2011.02561.x>.

Cameron, E.Z., du Toit, J.T., 2007. Winning by a neck: tall giraffes avoid competing with shorter browsers. *Am. Nat.* 169, 130–135. <https://doi.org/10.1086/509940>.

Charles, G.K., Porensky, L.M., Riginos, C., Veblen, K.E., Young, T.P., 2017. Herbivore effects on productivity vary by guild: cattle increase mean productivity while wildlife reduce variability. *Ecol. Appl.* 27, 143–155.

Coe, M.J., Cumming, D.H.M., Phillipson, J., 1976. Biomass and production of large African herbivores in relation to rainfall and primary production. *Oecologia* 22, 341–354. <https://doi.org/10.1007/BF00345312>.

Coverdale, T.C., Boucher, P.B., Singh, J., Palmer, T.M., Goheen, J.R., Pringle, R.M., Davies, A.B., 2024. Herbivore regulation of savanna vegetation: Structural complexity, diversity, and the complexity–diversity relationship. *Ecological Monographs* 94 (4), e1624. <https://doi.org/10.1002/ecm.1624>.

Daskin, J.H., Stalmans, M., Pringle, R.M., 2016. Ecological legacies of civil war: 35-year increase in savanna tree cover following wholesale large-mammal declines. *J. Ecol.* 104, 79–89. <https://doi.org/10.1111/1365-2745.12483>.

Davies, A.B., Asner, G.P., 2019. Elephants limit aboveground carbon gains in African savannas. *Glob. Chang. Biol.* 25, 1368–1382. <https://doi.org/10.1111/gcb.14585>.

Dos Reis, A.A., Werner, J.P.S., Silva, B.C., Figueiredo, G.K., Antunes, J.F.G., Esquerdo, J.C., Coutinho, A.C., Lamparelli, R.A.C., Rocha, J.V., Magalhães, P.S.G., 2020. Monitoring pasture aboveground biomass and canopy height in an integrated crop-livestock system using textural information from PlanetScope imagery. *Remote Sens.* 12, 2534.

Drusch, M., Del Bello, U., Carlier, S., Colin, O., Fernandez, V., Gascon, F., Hoersch, B., Isola, C., Laberinti, P., Martimort, P., Meygret, A., Spoto, F., Sy, O., Marchese, F., Bargellini, P., 2012. Sentinel-2: ESA's optical high-resolution Mission for GMES operational services. *Remote Sens. Environ.* 120, 25–36. <https://doi.org/10.1016/j.rse.2011.11.026>.

Farwell, L.S., Gudex-Cross, D., Anise, I.E., Bosch, M.J., Olah, A.M., Radeloff, V.C., Razenková, E., Rogova, N., Silveira, E.M.O., Smith, M.M., et al., 2021. Satellite image texture captures vegetation heterogeneity and explains patterns of bird richness. *Remote Sens. Environ.* 253, 112175.

February, E.C., Higgins, S.I., Bond, W.J., Swemmer, L., 2013. Influence of competition and rainfall manipulation on the growth responses of savanna trees and grasses. *Ecol* 94, 1155–1164. <https://doi.org/10.1890/12-0540.1>.

Fornara, D.A., Du Toit, J.T., 2008. Level interactions between ungulate browsers and woody plants in an African community savanna dominated by palatable-spinescent Acacia trees. *J. Arid Environ.* 72, 534–545. <https://doi.org/10.1016/j.jaridenv.2007.07.010>.

Friedlingstein, P., O'Sullivan, M., Jones, M.W., Andrew, R.M., Bakker, D.C.E., Hauck, J., Landschützer, P., Le Quéré, C., Luijckx, I.T., Peters, G.P., et al., 2023. Global carbon budget 2023. *Earth Syst. Sci. Data* 15, 5301–5369. <https://doi.org/10.5194/essd-15-5301-2023>.

Fundisi, E., Musakwa, W., Ahmed, F.B., Tesfamichael, S.G., 2020. Estimation of woody plant species diversity during a dry season in a savanna environment using the spectral and textural information derived from WorldView-2 imagery. *PLoS One* 15, e0234158. <https://doi.org/10.1371/journal.pone.0234158>.

Funk, C., Peterson, P., Landsfeld, M., Pedreros, D., Verdin, J., Shukla, S., Husak, G., Rowland, J., Harrison, L., Hoell, A., et al., 2015. The climate hazards infrared precipitation with stations—a new environmental record for monitoring extremes. *Sci. Data* 2, 1–21. <https://doi.org/10.1038/sdata.2015.66>.

Georgiadis, N.J., Olwero, J.G.N., Ojwang, G., Romanach, S.S., 2007. Savanna herbivore dynamics in a livestock-dominated landscape: I. Dependence on land use, rainfall, density, and time. *Biol. Conserv.* 137, 461–472. <https://doi.org/10.1016/j.biocon.2007.03.005>.

Gobush, K.S., Edwards, C.T., Balfour, D., Wittemyer, G., Maisels, F., Taylor, R.D., 2021. *Loxodonta africana*. The IUCN Red List of Threatened Species 2021: e. T181008073A181022663.

Goheen, J.R., Palmer, T.M., Charles, G.K., Helgen, K.M., Kinyua, S.N., Maclean, J.E., Turner, B.L., Young, H.S., Pringle, R.M., 2013. Piecewise disassembly of a large-herbivore community across a rainfall gradient: the UHURU experiment. *PLoS One* 8, e55192.

Goheen, J.R., Augustine, D.J., Veblen, K.E., Kimuyu, D.M., Palmer, T.M., Porensky, L.M., Pringle, R.M., Ratnam, J., Riginos, C., Sankaran, M., et al., 2018. Conservation lessons from large-mammal manipulations in east African savannas: the KLEE, UHURU, and GLADE experiments. *Ann. N. Y. Acad. Sci.* 1429, 31–49.

Gordijn, P.J., Rice, E., Ward, D., 2012. The effects of fire on woody plant encroachment are exacerbated by succession of trees of decreased palatability, 14, pp. 411–422. <https://doi.org/10.1016/j.ppees.2012.09.005>.

Gorelick, N., Hancher, M., Mike Dixon, M., Ilyushchenko, S., Thau, D., Moore, R., 2017. Google earth engine: planetary-scale geospatial analysis for everyone. *Remote Sens. Environ.* 202, 18–27. <https://doi.org/10.1016/j.rse.2017.06.031>.

Haralick, R.M., Shanmugam, K., Dinstein, I.H., 1973. Textural features for image classification. *IEEE Trans. Syst. Man.* 610–621.

Hoffer, R.M., Johannsen, C.J., 1969. Ecological potentials in spectral signature analysis. *Remote Sens. Ecol.* 1, 1–16.

Holdo, R.M., Sinclair, A.R.E., Dobson, A.P., Metzger, K.L., Bolker, B.M., Ritchie, M.E., Holt, R.D., 2009. A disease-mediated trophic cascade in the Serengeti and its implications for ecosystem C. *PLoS Biol.* 7, e1000210. <https://doi.org/10.1371/journal.pbio.1000210>.

Huete, A.R., Justice, C., Liu, H., 1994. Development of vegetation and soil indices for MODIS-EOS. *Remote Sens. Environ.* 49, 224–234.

Irob, K., Blaum, N., Tjetjen, B., 2024. Navigating uncertainty: managing herbivore communities enhances savanna ecosystem resilience under climate change. *J. Appl. Ecol.* 61, 145–157. <https://doi.org/10.1111/1365-2664.14573>.

Kacic, P., Kuenzer, C., 2022. Forest biodiversity monitoring based on remotely sensed spectral diversity—a review. *Remote Sens.* 14 (21), 5363. <https://doi.org/10.3390/rs14215363>.

Kambatuku, J.R., Cramer, M.D., Ward, D., 2011. Savanna tree-grass competition is modified by substrate type and herbivory. *J. Veg. Sci.* 22, 225–237. <https://doi.org/10.1111/j.1654-1103.2010.01239.x>.

Kibet, S., Nyangito, M., MacOpio, L., Kenfack, D., 2021. Savanna woody plants responses to mammalian herbivory and implications for management of livestock-wildlife landscape. *Ecol. Solut. Evid.* 2, e12083.

Levick, S.R., Asner, G.P., Kennedy-Bowdoin, T., Knapp, D.E., 2009. The relative influence of fire and herbivory on savanna three-dimensional vegetation structure. *Biol. Conserv.* 142, 1693–1700.

Mramba, R.P., 2021. Browsing behaviour of impala, *Aepyceros melampus* in two contrasting savannas. *Glob. Ecol. Conserv.* 30, e01770. <https://doi.org/10.1016/j.gecco.2021.e01770>.

Nasseri, N.A., McBryer, L.D., Schulte, B.A., 2011. The impact of tree modification by African elephant (*Loxodonta africana*) on herpetofaunal species richness in northern Tanzania. *Afr. J. Ecol.* 49, 133–140. <https://doi.org/10.1111/j.1365-2028.2010.01238.x>.

NICFI, 2022. Norway's International Climate and Forest Initiative (NICFI). Kongens Gate 20, Oslo. <https://www.nicfi.no/>.

O'Connor, D.A., Butt, B., Foufopoulos, J.B., 2015. Foraging ecologies of giraffe (*Giraffa camelopardalis reticulata*) and camels (*Camelus dromedarius*) in northern Kenya: effects of habitat structure and possibilities for competition? *Afr. J. Ecol.* 53, 183–193. <https://doi.org/10.1111/aje.12188>.

Ogutu, J.O., Kuloba, B., Piepho, H.-P., Kanga, E., 2017. Wildlife population dynamics in human-dominated landscapes under community-based conservation: the example of Nakuru wildlife conservancy, Kenya. *PLoS One* 12, e0169730. <https://doi.org/10.1371/journal.pone.0169730>.

Olson, D.M., Dinerstein, E., Wikramanayake, E.D., Burgess, N.D., Powell, G.V.N., Underwood, E.C., D'amico, J.A., Itoua, I., Strand, H.E., Morrison, J.C., et al., 2001. Terrestrial ecoregions of the world: a new map of life on EarthA new global map of terrestrial ecoregions provides an innovative tool for conserving biodiversity. *BioScience* 51, 933–938. [https://doi.org/10.1641/0006-3568\(2001\)051\[0933:TEOTWA\]2.0.CO;2](https://doi.org/10.1641/0006-3568(2001)051[0933:TEOTWA]2.0.CO;2).

Pandey, P., Kington, J., Kanwar, A., Curdoglo, M., 2021. Addendum to Planet Basemaps Product Specification. NICFI Basemaps.

Petrou, Z.I., Tarantino, C., Adamo, M., Blonda, P., Petrou, M., 2012. Estimation of Vegetation Height through Satellite Image Texture Analysis, in: Proceedings of the International Archives of the Photogrammetry, Remote Sensing and Spatial Information Sciences, XXII ISPRS Congress, Melbourne, B8.

Planet Labs PBC, 2020–2023. Planet application program Interface: in space for life on Earth. Planet <https://api.planet.com>. License. <https://university.planet.com/nicfi-re-sources/1219786>.

R Core Team, 2023. R: A Language and Environment for Statistical Computing. R Foundation for Statistical Computing, Vienna, Austria. <https://www.R-project.org/>.

Ripple, W.J., Newsome, T.M., Wolf, C., Dirzo, R., Everatt, K.T., Galetti, M., Hayward, M.W., Kerley, G.I.H., Levi, T., Lindsey, P.A., Macdonald, D.W., Malhi, Y., Painter, L.E., Sandom, C.J., Terborgh, J., van Valkenburgh, B., 2015. Collapse of the world's largest herbivores. *Sci. Adv.* 1, e1400103. <https://doi.org/10.1126/sciadv.1400103>.

Rouse, J.W., Haas, R.H., Schell, J.A., Deering, D.W., et al., 1974. Monitoring Vegetation Systems in the Great Plains with ERTS, 351. NASA Special Publication, p. 309.

Rubenstein, D., Mackey, B.L., Davidson, Z., Kébédé, F., King, S., 2016. *Equis grevyi*. The IUCN Red List of Threatened Species 2016: e. T7950A89624491.

Sankaran, M., Ratnam, J., Hanan, N., 2008. Woody cover in African savannas: the role of resources, fire and herbivory. *Glob. Ecol. Biogeogr.* 17, 236–245. <https://doi.org/10.1111/j.1466-8238.2007.00360.x>.

Searchinger, T.D., Estes, L., Thornton, P.K., Beringer, T., Notenbaert, A., Rubenstein, D., Heimlich, R., Licker, R., Herra, M., 2015. High carbon and biodiversity costs from converting Africa's wet savannahs to cropland. *Nat. Clim. Chang.* 5, 481–486. <https://doi.org/10.1038/nclimate2584>.

Shannon, C.E., 1948. A mathematical theory of communication. *Bell Syst. Tech. J.* 27, 379–423. <https://doi.org/10.1002/j.1538-7305.1948.tb01338.x>.

Sorokina, H.E., Nunes, M.H., Heiskanen, J., Munyao, M., Mwang'ombe, J., Pellikka, P., Raumonen, P., Maeda, E.E., 2024. East African megafauna influence on vegetation structure permeates from landscape to tree level scales. *Ecol. Inform.* 79, 102435. <https://doi.org/10.1016/j.ecoinf.2023.102435>.

Staver, A.C., Archibald, S., Levin, S.A., 2011. The global extent and determinants of savanna and forest as alternative biome states. *Sci* 334, 230–232. <https://doi.org/10.1126/science.1210465>.

Staver, A.C., Abraham, J.O., Hempson, G.P., Karp, A.T., Faith, J.T., 2021. The past, present, and future of herbivore impacts on savanna vegetation. *J. Ecol.* 109, 2804–2822. <https://doi.org/10.1111/1365-2745.13685>.

Szantoi, Z., Strobl, P., 2019. Copernicus Sentinel-2 calibration and validation. *Europ. J. Remote Sens.* 52, 253–255. <https://doi.org/10.1080/22797254.2019.1582840>.

Torresani, M., Rossi, C., Perrone, M., Hauser, L.T., Féret, J.-B., Moudrý, V., Simova, P., Ricotta, C., Foody, G.M., Kacic, P., Lucieer, A., Rocchini, D., Lausch, A., 2024. Reviewing the Spectral Variation Hypothesis: Twenty years in the tumultuous sea of biodiversity estimation by remote sensing. *Ecological Informatics* 80, 102702. <https://doi.org/10.1016/j.ecoinf.2024.102702>.

Wells, H.B.M., Crego, R.D., Opedal, Ø.H., Khasoha, L.M., Alston, J.M., Reed, C.G., Weiner, S., Kurukura, S., Hassan, A.A., Namoni, M., et al., 2021. Experimental evidence that effects of megaherbivores on mesoherbivore space use are influenced by species' traits. *J. Anim. Ecol.* 90, 2510–2522.

Wigley, B.J., Augustine, D.J., Coetsee, C., Ratnam, J., Sankaran, M., 2020. Grasses continue to trump trees at soil carbon sequestration following herbivore exclusion in a semiarid African savanna. *Ecol* 101, e03008. <https://doi.org/10.1002/ecy.3008>.

Wigley-Coetsee, C., Strydom, T., Govender, D., Thompson, D.I., Govender, N., Botha, J., Simms, C., Manganyi, A., Kruger, L., Venter, J., et al., 2022. Reflecting on research produced after more than 60 years of exclosures in the Kruger National Park. In: KOEDOE-African Protected Area Conservation and Science, 64, p. 1674.

Wood, E.M., Pidgeon, A.M., Radloff, V.C., Keuler, N.S., 2012. Image texture as a remotely sensed measure of vegetation structure. *Remote Sens. Environ.* 121, 516–526.

Young, T.P., Okello, B.D., Kinyua, D., Palmer, T.M., 1997. KLEE: A long-term multi-species herbivore exclusion experiment in Laikipia, Kenya. *Afr J Range Forage Sci* 14, 94–102. <https://doi.org/10.1080/10220119.1997.9647929>.